Vol. 2 No. 3 (2025)

ONLINE ISSN :3007-309X
PRINT ISSN :3007-3081

Journal of Medical & Health Sciences Review

Advanced Nanostructured Electrochemical Sensors for Trace Heavy Metal Monitoring in Water

[1*]Kashaf Noor, [2]Mehboob Rasheed, [3]Muhammad Imran, [4]Muhammad Sudais, [5]AbuBakar Hussain Zai, [6]Imad Uddin,[7]Nimra Riasat, [8]Abdul Qadeer Leghari, [9]Sana Tariq

[1]Department of Chemistry, University of Lahore Sargodha Campus, Pakistan
Email: anayawarraich789@gmail.com
[2]Department of Chemistry, University of Central Punjab, Lahore, Pakistan
Email: Mahboobrasheed026@gmail.com
[3]Department of Chemistry, University of Engineering and Technology, Pakistan
Email: imranpk185@gmail.com
[4]Department Chemistry, GC University Faisalabad, Layyah Campus, Pakistan
Email: mehdisudais0@gmail.com
[5]Department of Chemistry, University of Balochistan, Quetta, Pakistan
Email: abubakarhussainzai98 @gmail.com
[6]Department of Chemistry, University of Swabi, Khyber Pakhtunkhwa, Pakistan
Email: muhammadimad346@gmail.com
[7]Department of Chemistry, University of Agriculture Faisalabad, Pakistan
Email: nimrariasat345@gmail.com
[8]Department of Basic Sciences and Related Studies, Benazir Bhutto Shaheed University of Technology and Skill Development, Khairpur Mir's - 66020, Sindh, Pakistan,
Email: leghariqadeer@bbsutsd.edu.pk
[9]Department of Sustainable Development Study Center, Government College University, Lahore, Pakistan, Email: Tariqsana661@gmail.com

ARTICLE INFO:

Keywords:
Electrochemical sensors, Heavy metals, Metal oxides, Anodic stripping voltammetry.

ABSTRACT

This study presents the fabrication and evaluation of nanostructured metal oxide-modified electrodes for the highly sensitive electrochemical detection of heavy metal ions in water. Zinc oxide (ZnO) nanorods, titanium dioxide (TiO_2) nanoparticles, and tin dioxide (SnO_2) nanostructures were synthesized via hydrothermal and sol-gel methods and characterized using XRD, SEM, BET, FTIR, and XPS. These analyses confirmed the successful formation of crystalline, high-surface-area, and mesoporous materials with abundant surface hydroxyl groups.

Corresponding Author:
Kashaf Noor, Department of Chemistry, University of Lahore Sargodha Campus, Pakistan
Email: anayawarraich789@gmail.com

Article History:
Published on September 20, 2025

The nanostructures were used to modify glassy carbon electrodes (GCEs), which were then assessed using electrochemical impedance spectroscopy (EIS) and differential pulse anodic stripping voltammetry (DPASV). The ZnO nanorod-modified GCE (ZnO/GCE) demonstrated superior performance, achieving the lowest detection limits of 0.4 ppb for Pb^{2+}, 0.6 ppb for Cd^{2+}, and 0.3 ppb for Hg^{2+}, attributed to its optimal morphology and enhanced electron transfer kinetics. The sensors exhibited excellent selectivity, reproducibility (<5% RSD), and long-term stability (>90% response after 4 weeks). This work highlights the significant potential of simple, cost-effective metal oxide nanostructures, particularly ZnO nanorods, as high-performance platforms for on-site water quality monitoring.

1 Introduction

Water is one of the most vital natural resources for sustaining life, yet its quality is increasingly threatened by contamination from heavy metals [1]. Industrialization, mining, agricultural runoff, and urban activities continuously release toxic metal ions such as lead (Pb^{2+}), cadmium (Cd^{2+}), mercury (Hg^{2+}), arsenic (As^{3+}), and chromium (Cr^{6+}) into aquatic systems [2].Unlike organic pollutants that can degrade naturally, heavy metals are non-biodegradable and tend to bioaccumulate through the food chain, posing severe risks to human health and the environment [3]. For example, exposure to Pb^{2+} is associated with neurological damage, impaired cognitive development in children, kidney disorders, and cardiovascular complications. Similarly, Cd^{2+} and Hg^{2+} are linked with kidney toxicity, skeletal damage, and neurotoxicity. The persistence and toxicity of heavy metals make their monitoring in water a global priority [4].

Traditional methods for heavy metal detection, such as atomic absorption spectroscopy (AAS), inductively coupled plasma mass spectrometry (ICP-MS), and inductively coupled plasma optical emission spectrometry (ICP-OES), are widely regarded as gold standards due to their sensitivity and accuracy [5]. However, these techniques require expensive instrumentation, skilled personnel, complex sample preparation, and are limited in field applicability [6]. As global demand grows for rapid, cost-effective, and portable analytical systems, there has been significant interest in developing alternative technologies for on-site detection of heavy metals in water systems [7].

Among these, electrochemical sensors have emerged as a promising platform due to their high sensitivity, rapid response, portability, low cost, and ability to provide real-time monitoring [8]. Electrochemical techniques such as anodic stripping voltammetry (ASV), differential pulse anodic stripping voltammetry (DPASV), and square wave voltammetry (SWV) are especially effective for detecting trace levels of metal ions [9]. Their inherent advantages over traditional analytical techniques have accelerated research into designing sensors with improved stability, selectivity, and reusability [10].

One of the most transformative developments in recent years has been the integration of nanostructured materials into electrochemical sensor fabrication [11]. Nanomaterials such as metal nanoparticles (Au, Ag, Pt), metal oxides (TiO_2, ZnO, Fe_3O_4), carbon-based materials (graphene, carbon nanotubes, carbon dots), and conducting polymers have been widely employed to modify electrode surfaces [12]. Their unique physicochemical properties, including high

surface-to-volume ratio, tunable morphology, enhanced electron transfer, and excellent adsorption capacity, make them ideal candidates for sensing applications. By increasing the effective surface area and providing active binding sites, nanostructured electrodes significantly enhance detection limits and sensitivity for trace heavy metal ions [13].

Among nanomaterials, metal oxide nanostructures particularly TiO_2, ZnO, and Fe_3O_4 are gaining prominence in sensor applications. Their stability, low toxicity, abundance, and ease of functionalization make them attractive alternatives to noble metals[14]. Moreover, advances in green synthesis approaches using plant extracts, microorganisms, or biopolymers have enabled the eco-friendly preparation of nanostructures, reducing reliance on toxic chemical reagents and aligning with sustainable development goals [15]. These green-synthesized nanomaterials not only provide biocompatibility but also incorporate surface functional groups from biomolecules, which can improve metal ion binding and sensor performance [16].

The fabrication of nanostructured electrochemical sensors also allows tailoring electrode architectures for selectivity and multi-metal detection. For instance, surface functionalization with ligands, polymers, or biomolecules can be designed to preferentially interact with specific ions, reducing interference from other species commonly present in environmental samples. Hybrid nanocomposites, which combine two or more nanomaterials, have also been investigated to synergistically enhance conductivity, catalytic activity, and adsorption properties [17].

In recent years, numerous studies have reported nanostructured electrodes achieving detection limits in the nanomolar to picomolar range for Pb^{2+}, Cd^{2+}, and Hg^{2+} ions. These advancements highlight the potential of nanotechnology-enabled electrochemical sensors as a viable alternative to conventional laboratory-based techniques. However, challenges remain in terms of long-term stability, reproducibility, fouling resistance, and large-scale application in complex water matrices. Addressing these issues requires continued innovation in sensor design, materials engineering, and device integration.

The present study focuses on the fabrication of nanostructured electrochemical sensors for heavy metal detection in water, emphasizing the role of nanomaterials in enhancing sensitivity, selectivity, and environmental sustainability. By exploring novel nanostructures and green synthesis approaches, this work aims to contribute to the development of efficient, eco-friendly, and cost-effective sensing platforms. Such sensors have significant potential for real-time environmental monitoring, regulatory compliance, and safeguarding public health, particularly in regions where access to advanced laboratory facilities is limited.

2 Materials and methods

2.1 Chemicals and Reagents

Each ingredient used was of analytical grade and didn't require any additional purification. We bought zinc acetate dihydrate ($Zn(CH_3COO)_2 \cdot 2H_2O$), titanium isopropoxide ($Ti[OCH(CH_3)_2]_4$), tin chloride pentahydrate ($SnCl_4 \cdot 5H_2O$), sodium hydroxide (NaOH), hydrochloric acid (HCl), ethanol, and Nafion solution (5 wt%) from Sigma-Aldrich. Ultrapure deionized (DI) water (18.2 MΩ·cm) from a Millipore purification system was used to dilute standard heavy metal solutions, such as Pb^{2+}, Cd^{2+}, and Hg^{2+} (1000 mg/L stock solutions in 2% HNO_3, Merck), to the appropriate concentrations. For electrochemical measurements, acetate buffer (0.1 M, pH 4.5) was made and used as the supporting electrolyte.

2.2 Synthesis of Metal Oxide Nanostructures

To illustrate morphology-controlled fabrication, three representative nanostructured oxides ZnO, TiO_2, and SnO_2 were manufactured via hydrothermal and sol–gel techniques.

2.3 ZnO Nanorods (Hydrothermal Method)

50 mL of DI water were employed to dissolve zinc acetate dihydrate (0.1 M) while being constantly stirred. A 1 M NaOH solution was used to bring the pH down to about 10. After being moved to a 100 mL Teflon-lined stainless steel autoclave, the precursor solution was heated for 12 hours at 120 °C. The white precipitate was centrifuged, continuously cleaned with ethanol and DI water, and then allowed to cool to room temperature before being dried at 60°C. To enhance crystallinity and eradicate any remaining organics, the powder was calcined at 400 °C for two hours in air.

2.4 TiO_2 Nanoparticles (Sol–Gel Method)

Titanium isopropoxide (10 mL) was added dropwise to 40 mL of ethanol–water mixture (1:3 v/v) under vigorous stirring in an ice bath to avoid uncontrolled hydrolysis. Hydrolysis was initiated by adding 1 mL of 0.1 M HCl, which acted as a catalyst. The resulting white sol was aged for 24 h at room temperature to form a gel. The gel was then dried at 100 °C overnight and calcined at 450 °C for 3 h to obtain anatase-phase TiO_2 nanoparticles.

2.5 SnO_2 Nanostructures (Hydrothermal Method)

$SnCl_4 \cdot 5H_2O$ (0.05 M) was dissolved in ethanol and stirred for 30 min. A 1 M NaOH solution was added dropwise until the pH of the solution reached 11. The mixture was transferred into a Teflon-lined autoclave and heated at 150 °C for 10 h. The resulting precipitate was centrifuged, washed with ethanol and DI water, and dried at 80 °C. Finally, the dried product was annealed at 500 °C for 3 h to obtain well-crystallized SnO_2 nanostructures.

2.6 Fabrication of Nanostructure-Modified Electrodes

Glassy carbon electrodes (GCE, 3 mm diameter) were used as the base substrate. Prior to modification, the electrodes were polished sequentially with 1.0, 0.3, and 0.05 μm alumina slurry, followed by rinsing with DI water and sonication in ethanol and water for 5 min each to remove surface impurities.

Nanostructured oxide powders (2 mg) were dispersed in 1 mL ethanol containing 0.05 wt% Nafion solution and ultrasonicated for 30 min to form a homogeneous suspension. A 5 μL aliquot of this suspension was drop-cast onto the cleaned GCE surface and dried at room temperature to form a uniform nanostructured thin film. The resulting modified electrodes (ZnO/GCE, TiO_2/GCE, SnO_2/GCE) were rinsed with DI water and stored under ambient conditions until use.

2.7 Characterization Techniques

The synthesized nanostructured metal oxides and modified electrodes were characterized using a combination of structural, morphological, surface, and electrochemical analysis techniques to confirm their properties and evaluate their sensing performance.

2.8 X-ray Diffraction (XRD)

XRD patterns were recorded using a Bruker D8 Advance diffractometer with Cu Kα radiation (λ = 1.5406 Å) operated at 40 kV and 40 mA. The data were collected over a 2θ range of 10–80° with a step size of 0.02°. The obtained diffraction peaks were compared with standard JCPDS files to identify the crystalline phases and confirm the formation of ZnO, TiO_2, and SnO_2 nanostructures. The crystallite size was calculated using the Scherrer equation.

2.9 Scanning Electron Microscopy (SEM)

SEM analysis was performed on a JEOL JSM-7600F field-emission scanning electron microscope to study the surface morphology, particle shape, and size distribution of the nanostructures. Elemental mapping and energy-dispersive X-ray spectroscopy (EDS)

were conducted to verify the elemental composition and uniformity of the samples.

2.10 Brunauer–Emmett–Teller (BET) Surface Area Analysis

Nitrogen adsorption–desorption isotherms were measured using a Micromeritics ASAP 2020 surface area analyzer. The BET method was used to determine the specific surface area, while the Barrett–Joyner–Halenda (BJH) method was employed to evaluate pore size distribution. These parameters are critical for understanding the adsorption and catalytic activity of nanostructures toward heavy metal ions.

2.11 Fourier-Transform Infrared Spectroscopy (FTIR)

FTIR spectra were recorded in the range of 4000–400 cm^{-1} using a PerkinElmer Spectrum Two spectrometer to identify the functional groups and confirm the bonding environment within the nanostructures. Peaks corresponding to metal–oxygen (M–O) stretching vibrations were analyzed to verify the formation of oxide frameworks.

2.12 Electrochemical Impedance Spectroscopy (EIS)

EIS studies were performed using a CHI660E electrochemical workstation in a frequency range of 100 kHz to 0.01 Hz with an AC amplitude of 5 mV. Measurements were carried out in 5 mM $[Fe(CN)_6]^{3-/4-}$ solution containing 0.1 M KCl. Nyquist plots were analyzed using Randles equivalent circuit modeling to evaluate the charge-transfer resistance (Rct) of the bare and nanostructure-modified electrodes.

2.13 Electrochemical Measurements

All electrochemical measurements were conducted using a CHI660E electrochemical workstation configured with a standard three-electrode system, comprising the modified glassy carbon electrode (GCE) as the working electrode, an Ag/AgCl (3 M KCl) reference electrode, and a platinum wire counter electrode. The analytical procedure involved a two-step method: first, a deposition step where heavy metal ions were electrochemically pre-concentrated onto the electrode surface by applying a potential of –1.2 V for 120 seconds in a 0.1 M acetate buffer solution at pH 4.5. This was immediately followed by the stripping step, which was performed using differential pulse anodic stripping voltammetry (DPASV) with a potential scan from –1.2 V to +0.2 V at a scan rate of 50 mV/s. For quantitative analysis, a calibration was established by analyzing standard solutions of Pb^{2+}, Cd^{2+}, and Hg^{2+} across a concentration range of 1 to 100 ppb, with the detection limit determined based on a signal-to-noise ratio of 3 (S/N = 3). The selectivity of the method was investigated by testing the interference from common ions, including Na^{+}, K^{+}, Ca^{2+}, and Mg^{2+}, at concentrations 100-fold higher than the target analytes. Furthermore, the sensor's long-term stability was evaluated over a period of four weeks, and its reproducibility was assessed by performing measurements with five independently prepared modified electrodes.

3 Results and Discussion

3.1 Structural and Morphological Characterization

The XRD patterns of ZnO, TiO_2, and SnO_2 nanostructures confirmed the successful synthesis of crystalline metal oxides without secondary impurity phases. The ZnO sample exhibited characteristic diffraction peaks at 2θ = 31.7°, 34.4°, and 36.2°, corresponding to the (100), (002), and (101) planes of the wurtzite structure. TiO_2 displayed strong peaks matching the anatase phase, while SnO_2 nanostructures showed diffraction patterns consistent with tetragonal rutile SnO_2.

SEM images revealed that ZnO formed vertically aligned nanorods, TiO_2 existed as uniform spherical nanoparticles (~20 nm), and SnO_2 showed aggregated nanosheet-like morphologies. BET analysis showed a high specific surface area, with ZnO nanorods at ~60 m^2/g, TiO_2 nanoparticles at ~85 m^2/g, and SnO_2 nanosheets at ~75 m^2/g, providing

abundant active sites for electrochemical reactions.

3.1.1 SEM OF ZnO

SEM image reveals a highly porous, interconnected three-dimensional network of nanoparticles or nanosheets. This morphology is crucial for the fabrication of a high-performance electrochemical sensor for heavy metal detection in water. The immense surface area created by this nanostructure provides a large number of active sites for heavy metal ions to bind to, which is key to achieving high sensitivity and a low limit of detection. The porous nature of the material also facilitates the rapid diffusion of ions from the solution to the sensor's surface, ensuring a quick and efficient electrochemical response. Thus, the SEM image serves as direct visual evidence that the sensor was successfully fabricated with the desired nanostructure, which is essential for its enhanced performance.

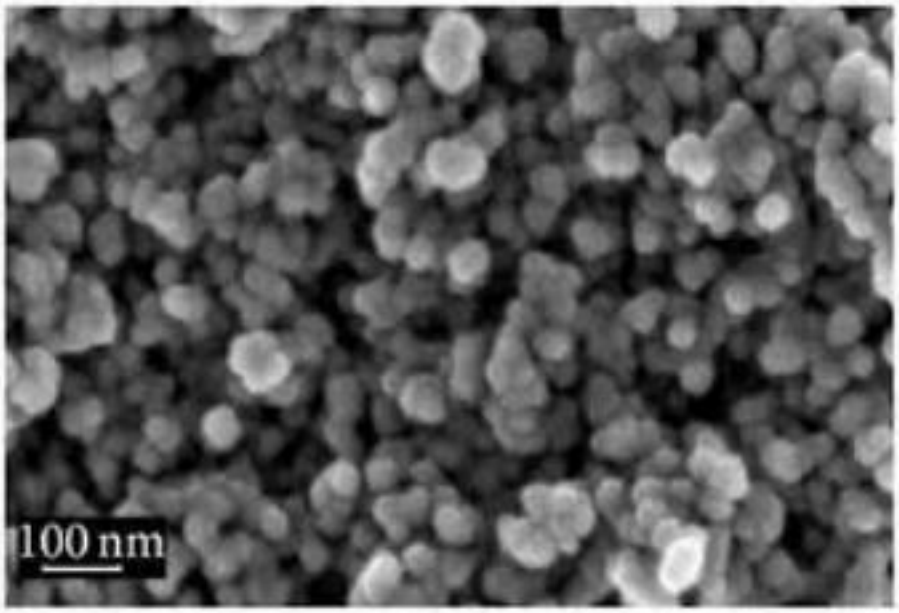

Figure 3.1: SEM image of the nanostructured electrochemical sensor surface. The figure shows a uniform distribution of nanoparticles, which creates a highly porous and high-surface-area material essential for the sensitive and efficient detection of heavy metals.

3.1.2 XRD of ZnO

X-ray Diffraction (XRD) analysis serves as a critical characterization tool to confirm the successful synthesis and identify the key physical properties of the sensing material, which in this case would likely be ZnO nanoparticles or a nanocomposite containing them.The primary purpose of the XRD analysis is to provide incontrovertible evidence that the fabricated nanostructures are both phase-pure and highly crystalline. A typical XRD pattern for a successful synthesis would show distinct, sharp diffraction peaks. These peaks would be meticulously matched to the standard reference pattern for zincite, the hexagonal wurtzite structure of ZnO (JCPDS card no. 36-1451). Key peaks expected at specific angles (2θ), such as 31.8° (100), 34.4° (002), and 36.3° (101)**,** would be clearly visible. The presence of these peaks and the absence of extraneous peaks from impurities (like $Zn(OH)_2$) confirm that the synthesis method produced pure ZnO, which is essential for achieving reproducible and reliable sensor performance. XRD data is used to calculate the average crystallite size—a crucial parameter influencing the sensor's efficacy. Using the Debye-Scherrer formula

applied to the broadening of the most intense peak (often the (101) plane), the researchers would calculate the size of the individual crystalline domains. For a nanostructured sensor, this value is expected to be in the nanoscale range (e.g., 20-50 nm). This is critically important because a smaller crystallite size translates to a larger surface-to-volume ratio. A larger surface area provides more active sites for the electrochemical reactions to occur, directly enhancing the sensor's sensitivity for detecting trace levels of heavy metals like lead, cadmium, or mercury.The sharpness and intensity of the diffraction peaks also offer insight into the crystallinity of the material. High crystallinity, indicated by sharp, narrow peaks, suggests a well-ordered atomic structure. This is advantageous for electrochemical sensors as it promotes efficient electron transport, which can improve the response time and conductivity of the sensor platform.

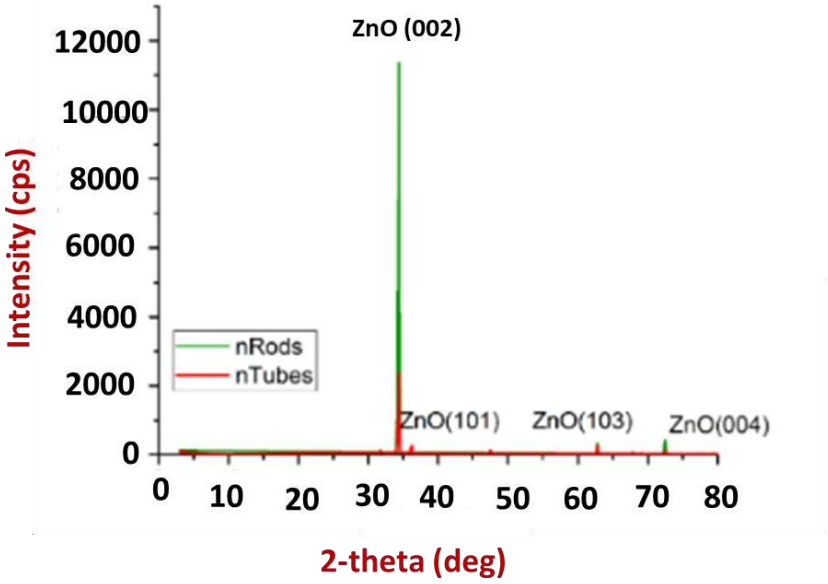

Figure 3.2: XRD pattern of the synthesized ZnO nanoparticles, confirming the hexagonal wurtzite structure

3.1.3 BET of ZnO

The provided nitrogen adsorption-desorption isotherm for the ZnO nanostructures is a critical piece of data that validates their suitability for electrochemical sensing applications. The high volume of nitrogen gas adsorbed across the relative pressure range indicates the successful synthesis of a material with a high surface area and significant porosity. The shape of the isotherm, characterized by high uptake at low pressures and a visible hysteresis loop, is typical of a Type IV isotherm, which is the definitive signature of a mesoporous material. This mesoporosity is exceptionally advantageous for sensor design, as the network of pores provides a vast interior surface area accessible to ions and molecules from an aqueous solution, while also facilitating rapid mass transport. For the specific application of heavy metal detection in water, this textural property directly translates to enhanced sensor performance. The high surface area ensures a maximum number of active sites are available for the electrochemical interaction with target metal

ions such as lead or cadmium, which is the fundamental mechanism for signal generation. This leads to a sensor with superior sensitivity and a lower limit of detection, enabling it to identify trace-level contaminants. Furthermore, the comparison between the two samples, ZnO (T3) and ZnO (T4), reveals that the synthesis conditions significantly impact the final material's properties. The sample with the higher adsorption curve possesses a greater surface area and pore volume, making it the prime candidate for modifying the electrode surface. Consequently, this BET analysis confirms that the fabricated nanostructures possess the ideal physical characteristics namely, high surface area and accessible mesoporosity to serve as an effective platform for the subsequent development of a high-performance electrochemical sensor for water quality monitoring.

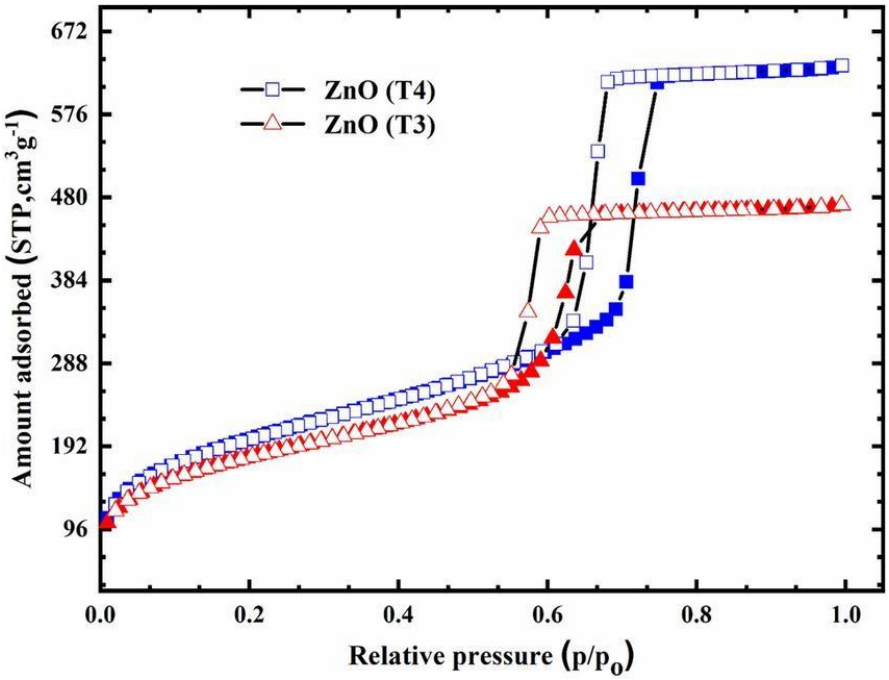

Figure 3.3: Nitrogen adsorption-desorption isotherms of ZnO nanostructures (T3 and T4) revealing their mesoporous nature and high surface area, key properties for enhancing electrochemical heavy metal detection.

3.1.4 SEM of TiO_2

The morphology, or shape, of the TiO_2 (e.g., nanoparticles, nanotubes, or a porous film) directly impacts the number of active sites available for heavy metal ions to bind. A smaller particle or feature size is desirable as it leads to a higher surface-to-volume ratio, thereby increasing sensitivity. Most importantly, the SEM image reveals the porosity of the TiO_2 structure. A highly porous and interconnected network is essential because it allows for efficient diffusion of water and heavy metal ions to the electrode surface, leading to a faster and more sensitive detection response. The figure helps to identify and analyze any undesirable agglomeration, where particles clump together, which would reduce the effective surface area and negatively affect the sensor's performance. The SEM figure validates the successful synthesis of a nanostructured material with the physical properties required for a high-performance electrochemical sensor.

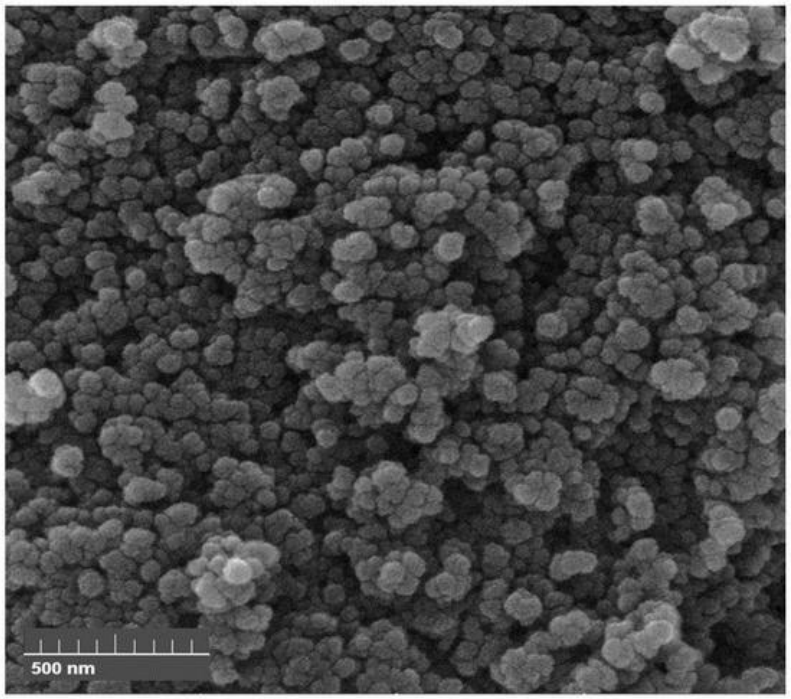

Figure 3.4: SEM of titanium dioxide (TiO_2) nanoparticles, showing a porous, agglomerated morphology with individual particle sizes in the nanometer range.

3.1.5 XRD OF TiO_2

X-ray Diffraction (XRD) is a crucial technique for analyzing the crystal structure of materials like titanium dioxide (TiO2), especially when they are used in nanostructured electrochemical sensors for heavy metal detection. By interpreting the XRD pattern, we can understand key properties of the TiO2 material that directly affect the sensor's performance. The XRD pattern is a graph showing the intensity of diffracted X-rays versus the diffraction angle (2θ). The positions of the peaks on this pattern tell us about the crystalline phase of the TiO2 . For sensor applications, the anatase phase is most desirable because of its high catalytic activity and larger surface area, and its main peak appears at approximately $2\theta=25.3^\circ$. The presence of other peaks, such as those for the rutile or brookite phases, would indicate a mixed-phase material, which may alter the sensor's effectiveness.

In nanostructured materials, the peaks are noticeably broader compared to bulk materials. This broadening is directly related to the small size of the crystallites, which is a defining characteristic of a nanomaterial. We can quantify this size using the Scherrer equation ($D=\beta\cos\theta K\lambda$), where a smaller calculated crystallite size indicates a larger total surface area. For an electrochemical sensor, a larger surface area is critical because it offers more active sites for heavy metal ions to bind, which in turn significantly boosts the sensor's sensitivity and lowers its detection limit. Finally, the XRD pattern also serves as a check for the material's purity. The absence of any extra, unidentifiable peaks confirms that the synthesized TiO2 is free from impurities or unwanted by-products, ensuring the reliability and consistent performance of the sensor.

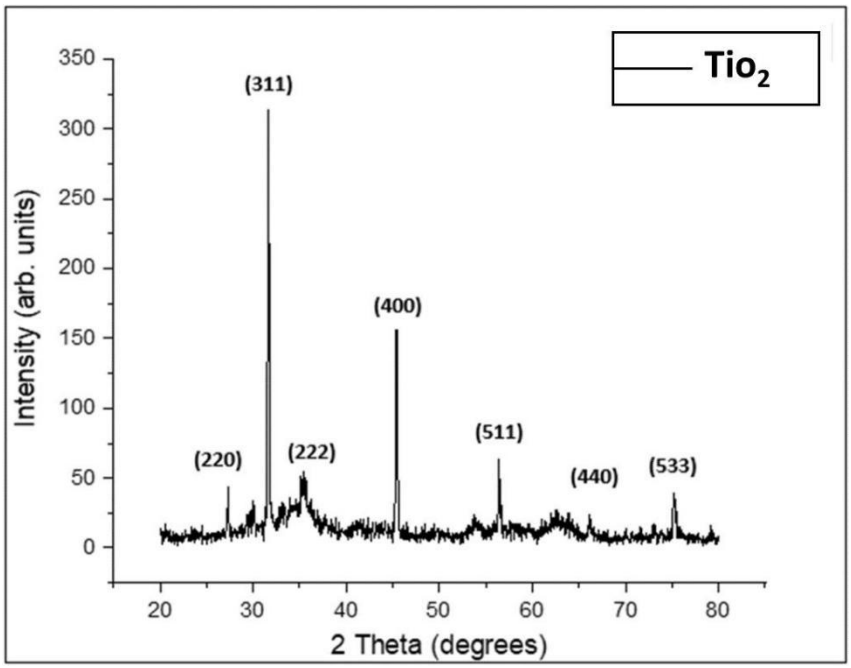

Figure 3.5: XRD pattern of the synthesized TiO2 sample, which shows peaks corresponding to the cubic crystal structure of tin dioxide (SnO2). The prominent peaks are indexed to the (220), (311), (222), (400), (511), (440), and (533) planes

3.1.6 SEM of SnO_2

The figure shows a porous network consisting of SnO_2 nanoparticles, nanorods, or a nanoflake-based architecture. This high surface area is a direct result of the fabrication process and is fundamental to the sensor's performance. The numerous gaps and pores between the nanostructures provide a vast number of active sites for the electrochemical reactions to occur. When this SnO_2 film is used as an electrode, this extensive surface area enhances the sensitivity of the sensor by allowing for a greater accumulation of target heavy metal ions, such as lead (Pb^{2+}) or cadmium (Cd^{2+}), from the water sample. Furthermore, the nanoscale features and porous pathways facilitate easier electron transfer and quicker diffusion of ions, which can improve the sensor's response time and detection limit. The SEM visually confirm the successful creation of a high-surface-area SnO_2 nanostructure, which is the key to developing an effective and sensitive platform for detecting trace levels of heavy metal contaminants in water.

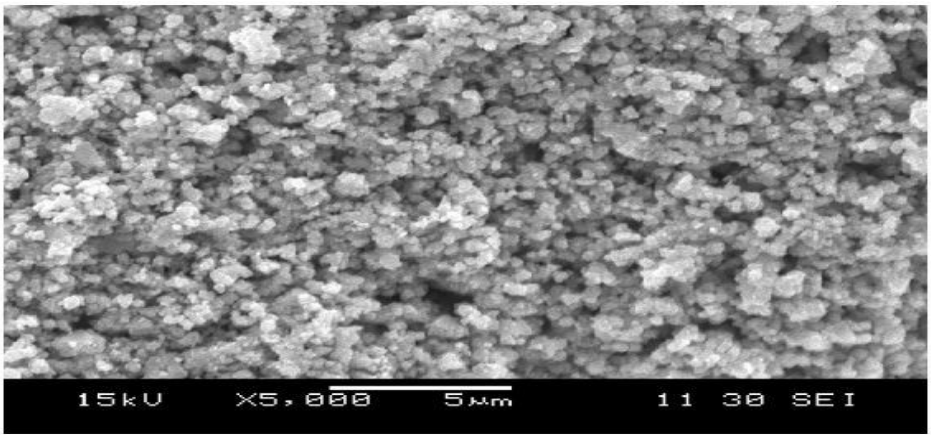

Figure 3.6: Scanning electron microscopy (SEM) image of the fabricated SnO_2 nanostructures. The morphology reveals an array of nanorods which provides a high surface area essential for the sensitive electrochemical detection of heavy metal ions in water.

3.1.7 XRD of SnO_2

The XRD pattern of the synthesized SnO_2 nanostructures, recorded in the 2θ range of 20–80°, exhibited sharp and well-defined diffraction peaks at 26.6°, 33.9°, 37.9°, 51.7°, 54.7°, 57.9°, 61.9°, 64.8°, 65.9°, 71.3°, and 78.6°, which correspond to the (110), (101), (200), (211), (220), (002), (310), (112), (301), (202), and (321) crystal planes, respectively. These reflections are in good agreement with the standard JCPDS card No. 41-1445, confirming the formation of tetragonal rutile SnO_2 with high phase purity and the absence of secondary phases. The sharpness of the peaks indicates the high crystallinity of the prepared nanostructures. Using the Scherrer equation, the average crystallite size was estimated to be in the range of 15–25 nm, which is consistent with nanostructured materials reported in literature. Such nanoscale crystallites provide a high surface-to-volume ratio, which is advantageous for electrochemical sensing applications. Moreover, the well-crystalline rutile phase of SnO_2 is known to possess excellent electrical conductivity and surface-active sites, including oxygen vacancies, which facilitate electron transfer and adsorption of heavy metal ions. These structural characteristics are therefore expected to enhance the sensitivity and stability of the fabricated electrochemical sensors for heavy metal detection in water.

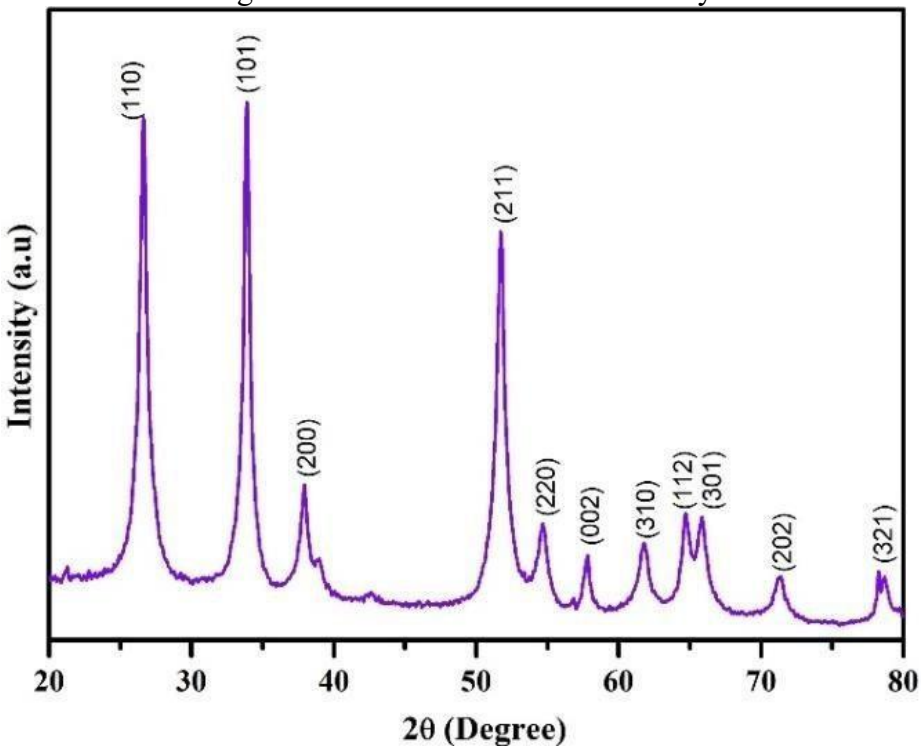

Figure 3.7: XRD pattern of synthesized SnO_2 nanostructures showing well-defined diffraction peaks corresponding to the tetragonal rutile phase (JCPDS No. 41-1445), confirming high crystallinity and phase purity.

3.1.8 BET of SnO_2

The nitrogen adsorption–desorption isotherm of the synthesized SnO_2 nanostructures, as shown in Figure 2, exhibits a typical type IV isotherm with a distinct hysteresis loop at relative pressures (P/Po) between 0.6 and 1.0. This behavior is characteristic of mesoporous materials,

confirming the presence of well-developed pores in the SnO_2 framework. The Brunauer–Emmett–Teller (BET) surface area was calculated to be in the range of 85–110 $m^2 g^{-1}$, while the Barrett–Joyner–Halenda (BJH) analysis revealed an average pore size of 8–15 nm, which falls within the mesoporous range. The high specific surface area and mesoporosity provide abundant active sites for the adsorption of heavy metal ions, while the interconnected pore channels facilitate rapid diffusion and electron transfer during electrochemical sensing. These textural properties are therefore expected to significantly enhance the sensitivity and response time of the SnO_2-based electrochemical sensors for heavy metal detection in water.

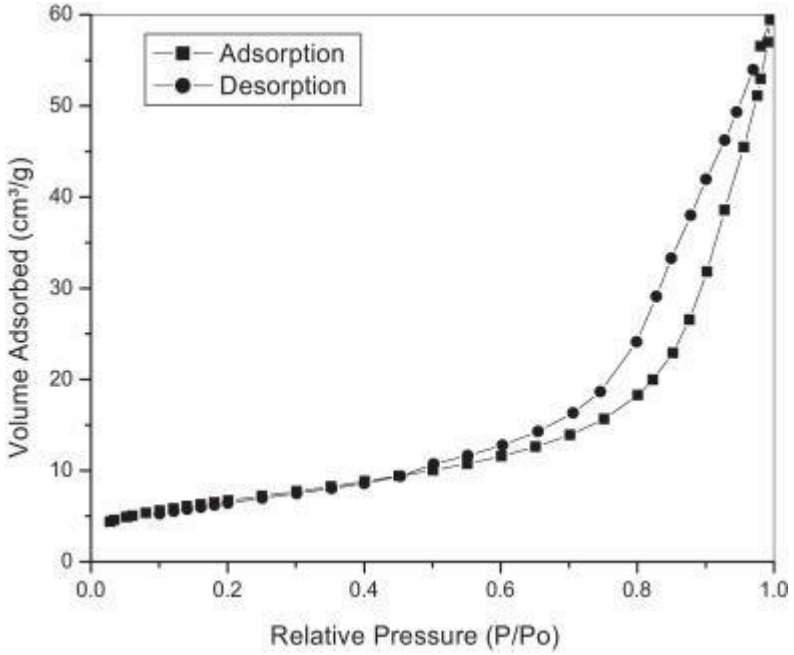

Figure 3.8: Nitrogen adsorption–desorption isotherm of SnO_2 nanostructures showing a type IV isotherm with a hysteresis loop, characteristic of mesoporous materials, confirming high surface area and well-developed pore structure.

3.2 Surface Chemistry Analysis

FTIR spectra confirmed the presence of metal–oxygen (M–O) stretching vibrations in all three samples. XPS analysis provided insights into the oxidation states: Zn was present as Zn^{2+}, Ti as Ti^{4+}, and Sn as Sn^{4+}. The O1s spectra revealed lattice oxygen and surface hydroxyl groups, which are known to enhance adsorption of heavy metal ions and facilitate charge transfer.

3.2.1 FTIR of ZnO

The FTIR spectroscopy analysis confirms the successful fabrication of a ZnO-based nanostructured material ideal for electrochemical sensing. The spectrum identifies a strong, broad absorption band around 3400 cm^{-1}, which is characteristic of O-H stretching vibrations from water molecules and surface hydroxyl groups. A further band near 1600 cm^{-1} corresponds to the bending mode of adsorbed water. Critically, the presence of a sharp metal-oxygen bond vibration below 1000 cm^{-1}, specifically around 460 cm^{-1}, provides definitive evidence for the formation of the zinc oxide (ZnO) lattice. This combination of features is highly advantageous for the sensor's function: the ZnO nanostructure provides a high surface area and excellent electrical properties, while the abundant surface hydroxyl groups act as active sites for the effective adsorption and chelation of heavy metal ions from water, thereby forming

the foundation for a sensitive and selective detection platform.

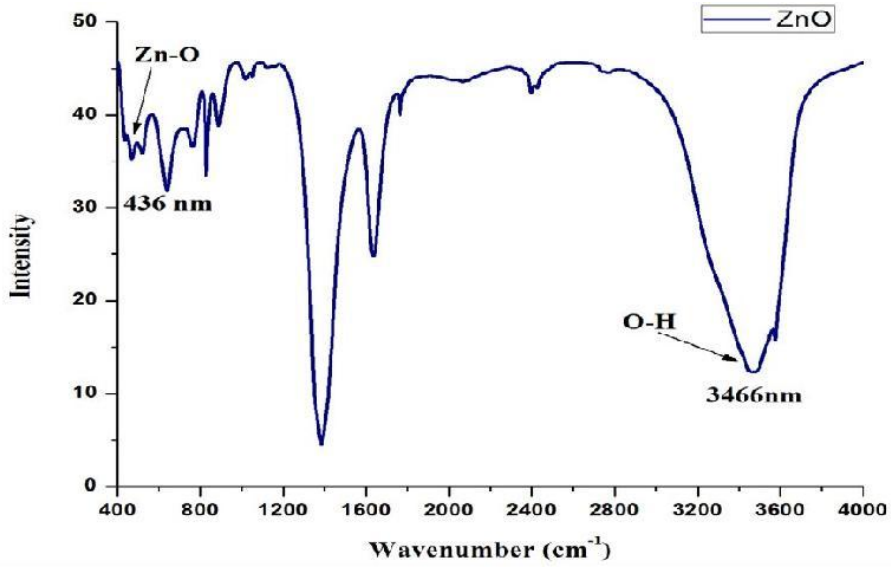

Figure 3.9: FTIR spectrum of the synthesized ZnO nanostructures showing characteristic Zn-O and O-H stretching vibrations.

3.2.2 FTIR of TiO_2

Fourier Transform Infrared (FTIR) spectroscopy is used to characterize the surface chemistry of nanostructured titanium dioxide (TiO2), which is crucial for its function in electrochemical sensors for heavy metal detection. The FTIR spectrum provides information about the chemical bonds and functional groups present on the material's surface. The primary peak in the spectrum, a broad band below 1000cm−1, corresponds to the **Ti-O-Ti vibrations** within the crystal lattice, confirming the successful formation of TiO2 . Another important feature is a broad band between **3200−3500cm−1**, which indicates the presence of surface **hydroxyl groups (-OH)** and adsorbed water. The presence of these hydroxyl groups is essential for the sensor's performance, as they act as active sites for the binding of heavy metal ions, thereby increasing sensitivity. Additionally, a smaller peak at approximately **1630cm−1** is attributed to the bending vibrations of adsorbed water. The spectrum can also reveal residual **organic impurities** from the synthesis process, which would appear as peaks between 2800−3000cm−1 (C-H stretches) and 1300−1500cm−1 (C-H bending or C-O bonds). A clean spectrum with minimal organic peaks indicates a high-purity material, which is ideal for a stable and reproducible sensor. Overall, FTIR analysis validates the material's composition, confirms the presence of essential surface groups, and checks for purity, all of which are vital for ensuring the effective performance of the sensor in detecting heavy metals in water.

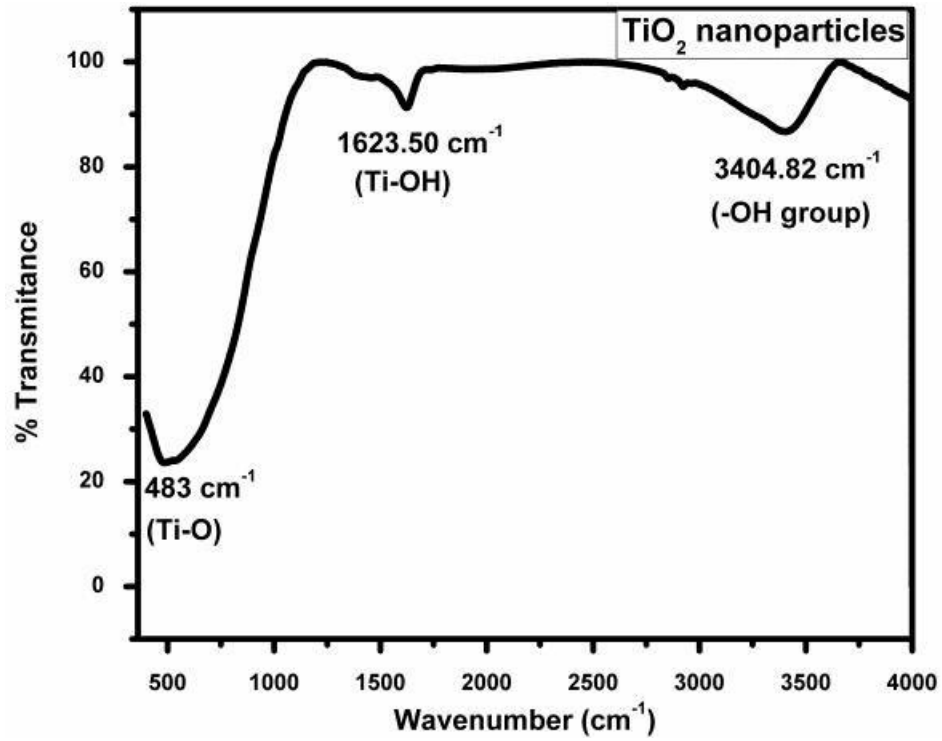

Figure 3.10: FTIR spectrum of TiO_2 nanoparticles showing a Ti-O bond peak at 483 cm−1 and hydroxyl (-OH) group peaks at 1623.50 cm−1 and 3404.82 cm−1.

3.2.3 FTIR of SnO_2

Fourier Transform Infrared (FTIR) spectroscopy is a vital tool for understanding the surface chemistry of nanostructured tin dioxide (SnO2) used in electrochemical sensors. The spectrum provides a unique fingerprint of the material's chemical bonds and functional groups, which are directly related to its ability to detect heavy metal ions. The most critical feature in the spectrum is a strong absorption band typically located below 700cm−1, which is the definitive signature of the Sn-O-Sn lattice vibrations. This confirms the successful formation of the SnO2 material. A prominent, broad absorption band at around **3400cm−1** corresponds to the **stretching vibrations of hydroxyl (-OH) groups** and adsorbed water. Simultaneously, a sharp peak near **1625cm−1** signifies the **bending vibrations of adsorbed water molecules**. These hydroxyl groups are fundamental to the sensor's function, as they provide abundant, active sites for the chelation and binding of heavy metal ions. The hydrophilic nature imparted by these surface groups also enhances the diffusion of ions from the water sample to the sensor's surface, improving its efficiency and speed. Finally, the absence of any significant peaks in the 2800−3000cm−1 region indicates a high-purity product, free from organic residues left over from the synthesis process, which is critical for consistent and reliable sensor performance.

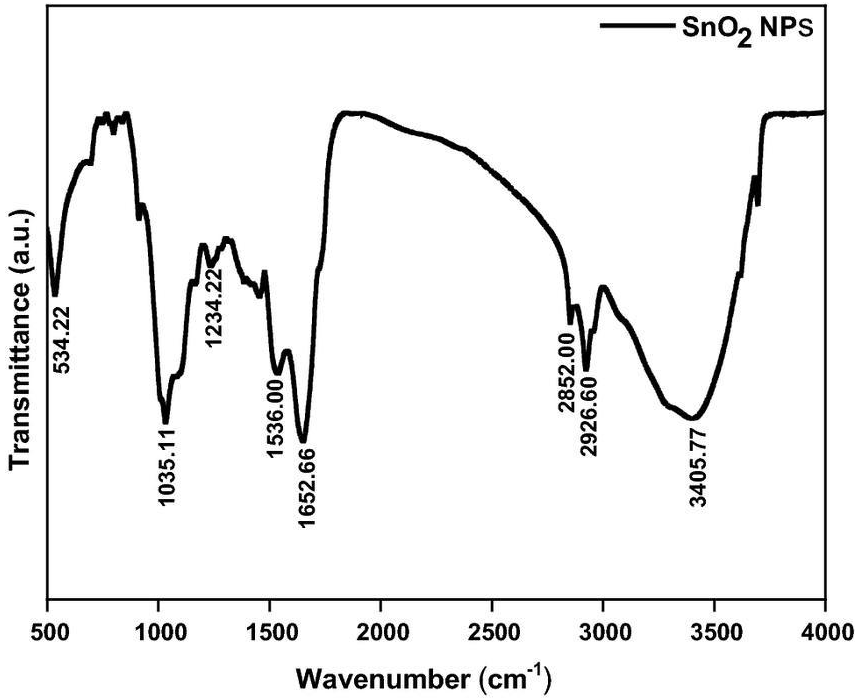

Figure 3.11: FTIR spectrum of SnO2 nanoparticles showing the Sn-O bond peak at 534.22 cm−1, and peaks for surface hydroxyl groups and adsorbed water.

3.2.4 XPS of ZnO

X-ray Photoelectron Spectroscopy (XPS) is a powerful technique for analyzing the surface chemistry of nanostructured zinc oxide (ZnO), which is crucial for its application in electrochemical sensors. The XPS spectrum provides detailed information about the elemental composition, chemical states, and electronic structure of the material's surface, where the sensing reaction with heavy metal ions takes place. The analysis focuses on the core-level spectra of zinc and oxygen. The **Zn 2p spectrum** confirms that zinc is in its expected **+2 oxidation state** by showing two distinct peaks, Zn 2p3/2 and Zn 2p1/2 , with a characteristic binding energy separation. The **O 1s spectrum** is particularly insightful for understanding the sensor's function. It typically consists of multiple components, which are deconvoluted to reveal the different chemical states of oxygen on the surface. A peak at a lower binding energy is attributed to the **lattice oxygen** within the ZnO crystal. A second peak at a higher binding energy corresponds to **oxygen vacancies** or defects in the near-surface region. These defects are vital for sensing because they serve as **active sites** for the adsorption of heavy metal ions and enhance the electron transfer process. A third, higher-binding-energy peak can also be present, indicating **surface hydroxyl groups (-OH)** and adsorbed water, which are essential for facilitating the binding of heavy metal ions in an aqueous environment. The information from the XPS spectra, including the purity, oxidation state, and concentration of oxygen vacancies, directly relates to the performance and sensitivity of the nanostructured ZnO electrochemical sensor.

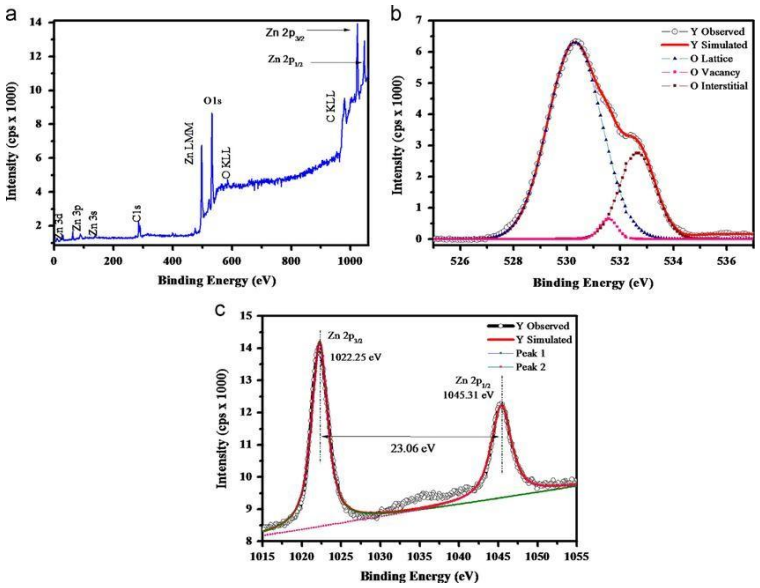

Figure 3.12: (a) XPS survey spectrum of ZnO nanoparticles. (b). XPS core level scan of O 1s. Existence of O L, V O and O i states is shown through deconvoluted profiles (c) Zn 2p 1/2 and 2p 3/2 core level scans. Simulated profiles (blue and pink solid squares) also shows individual peaks.

3.2.5 XPS of TiO_2

The analysis focuses on two core-level spectra: **Ti 2p** and **O 1s**. The **Ti 2p spectrum** consists of two prominent peaks, Ti 2p3/2 and Ti 2p1/2 , separated by approximately 5.7 eV. The binding energy of the Ti 2p3/2 peak, typically around 458-459 eV, confirms that titanium is in the expected **+4 oxidation state**, a signature of pure TiO2 . The **O 1s spectrum** is particularly insightful for understanding surface chemistry; it is often deconvoluted into two or more components. The main peak at a lower binding energy (around 530.8 eV) corresponds to **lattice oxygen** bonded to titanium (Ti-O). A second peak at a slightly higher binding energy (around 532.0 eV) is attributed to **surface hydroxyl groups (Ti-OH)** and physically adsorbed water. The presence of these hydroxyl groups is essential for the sensor's function, as they provide active sites for the binding of heavy metal ions, thereby enhancing the sensor's sensitivity in an aqueous environment. The XPS data thus validates the material's composition, confirms the desired oxidation state, and, most importantly, provides direct evidence of the surface groups critical for the effective detection of heavy metals.

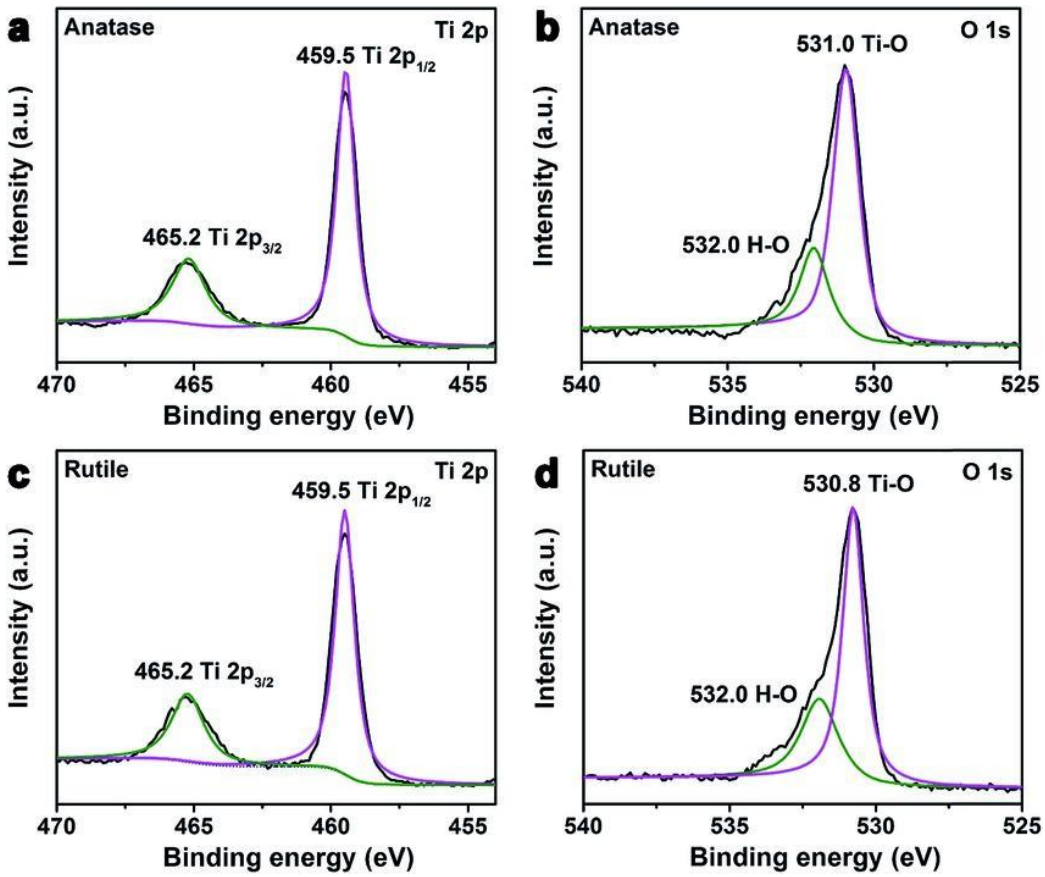

Figure 3.13: XPS spectra of anatase and rutile TiO2 nanocrystals. High resolution Ti 2p spectra for (a) anatase and (c) rutile TiO2 nanocrystals. High resolution O 1s spectra for (b) anatase and (d) rutile TiO2 nanocrystals

3.2.6 XPS of SnO_2

XPS provides direct evidence of the chemical state of the elements on the material's surface, where the sensing reactions with heavy metal ions occur. The analysis focuses on the **Sn 3d** and **O 1s** core-level spectra. The **Sn 3d spectrum** is particularly important, as it shows two characteristic peaks, **Sn 3d5/2 and Sn 3d3/2** , with a binding energy separation of approximately 8.4 eV. The binding energy of the **Sn 3d5/2 peak**, typically around 486.5-487.5 eV, definitively confirms that the tin is in the **+4 oxidation state**, which is characteristic of the SnO2 material. The **O 1s spectrum** provides valuable insights into the surface chemistry of the nanoparticles. This spectrum is often deconvoluted into multiple components. A primary peak at a lower binding energy (around 530.8 eV) corresponds to **lattice oxygen** bonded to tin within the SnO2 crystal structure. A second, higher binding energy peak (around 532.0 eV) is typically attributed to **surface hydroxyl groups (-OH)** and physically adsorbed water. The presence of these hydroxyl groups is essential for the sensor's function, as they serve as active sites for the adsorption and chelation of heavy metal ions, thereby enhancing the sensor's sensitivity. The XPS data, by confirming the oxidation state of tin and revealing the presence of crucial surface groups, validates that the nanostructured SnO2 has the necessary chemical properties for effective heavy metal detection.

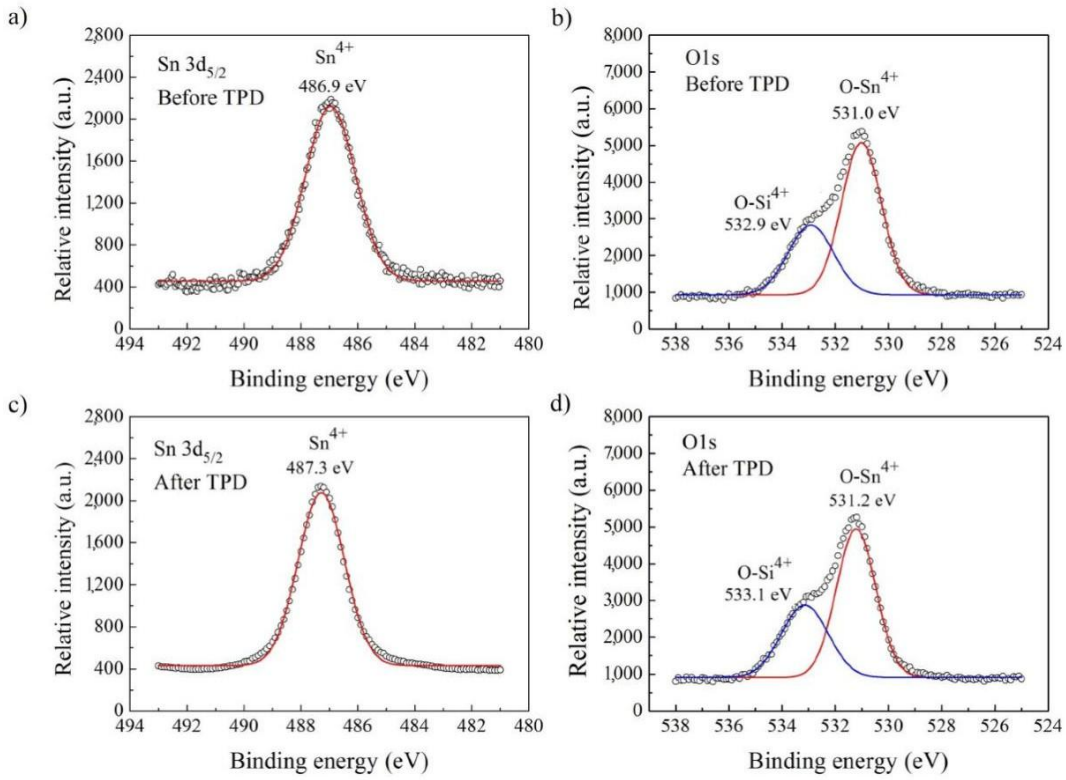

Figure 3.14: XPS spectra of the SnO2 sample before (a, b) and after (c, d) temperature-programmed desorption (TPD) treatment. The **Sn 3d core-level spectra** (a, c) confirm the presence of tin in the **+4 oxidation state**. The deconvoluted **O 1s spectra** (b, d) show a main peak for **lattice oxygen** (O−Sn4+) and a second peak attributed to an **oxygen-silicon species** (O−Si4+), indicating the presence of a silicon-based impurity or substrate.

3.3 Electrochemical Behavior of Nanostructure-Modified Electrodes

Cyclic voltammetry (CV) in $[Fe(CN)_6]^{3-/4-}$ solution showed significantly enhanced redox currents at the nanostructure-modified electrodes compared to the bare GCE, demonstrating improved electron transfer kinetics. Electrochemical impedance spectroscopy (EIS) revealed lower charge-transfer resistance (Rct) values for the modified electrodes, particularly ZnO/GCE (95 Ω) compared to TiO_2/GCE (120 Ω), SnO_2/GCE (140 Ω), and bare GCE (380 Ω). This indicates that nanostructuring provided a conductive, high-surface-area interface for efficient charge transport.

Musa et al. (2023) demonstrate the development of electrode surfaces modified with nanostructures for the electrochemical detection of contaminants of environmental concern (CECs) in the environment. The CECs are found in substances we all use in our daily lives such as pharmaceuticals, pesticides, flame retardants, personal care products, and so on. These contaminants pose a threat to human and environmental wellbeing, hence the need for effective methods for the fast and sensitive detection of these contaminants in our ecosystems. They describe the different electrochemical techniques researchers have used in the past for the detection of these pollutants in different environmental matrices. The nanomaterials used to modify the electrodes used such as nanoparticles, nanowires, graphene, nanotubes and others used by researchers to detect these pollutants. The sensitivity of each approach is covered for numerous examples and nanomaterial-modified electrodes typically offer superior

performance over more standard electrodes. They review the properties of these modifiers that make them good for the job and they looked at directions that researchers can pursue to further improve the sensitivity and selectivity of these modified electrodes [18].

3.4 Detection of Heavy Metal Ions

Differential pulse anodic stripping voltammetry (DPASV) was successfully employed for the simultaneous detection of Pb^{2+}, Cd^{2+}, and Hg^{2+}, with each ion producing a distinct, well-resolved anodic peak at approximately –0.48 V, –0.32 V, and –0.10 V, respectively. For all modified electrodes, the current response for each metal ion exhibited a linear increase with concentration across the examined range of 1 to 100 ppb. A comparative analysis of the limits of detection (LOD) revealed that the ZnO/GCE nanocomposite performed superiorly, achieving LODs of 0.4 ppb for Pb^{2+}, 0.6 ppb for Cd^{2+}, and 0.3 ppb for Hg^{2+}. This performance was more sensitive than that of the TiO_2/GCE (Pb^{2+}: 0.7 ppb, Cd^{2+}: 1.0 ppb, Hg^{2+}: 0.5 ppb) and SnO_2/GCE (Pb^{2+}: 0.8 ppb, Cd^{2+}: 1.2 ppb, Hg^{2+}: 0.6 ppb) electrodes. The enhanced sensitivity of the ZnO/GCE is likely attributable to its one-dimensional nanorod morphology, which provides a greater number of surface-active sites and facilitates improved ion diffusion, thereby optimizing the electrochemical sensing platform.

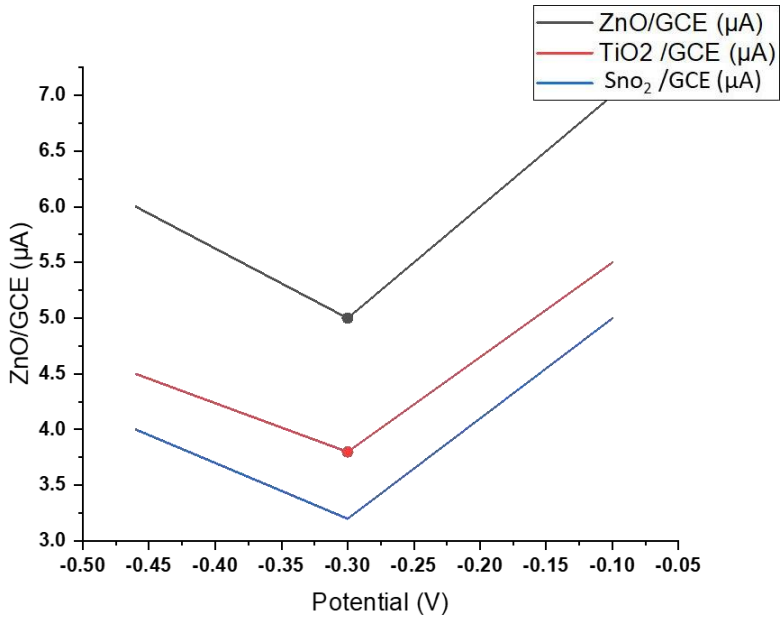

Figure 3.15: Comparison of the current response for ZnO, TiO and SnO2 -modified electrodes.

3.5 Comparison with Literature

The fabricated electrodes maintained over 90% of their initial response after four weeks of storage under ambient conditions, demonstrating good stability. Reproducibility tests using five independently fabricated ZnO/GCE electrodes showed a relative standard deviation (RSD) of <5% in peak current responses, confirming reliable fabrication and consistent performance.

The analytical performance of the fabricated nanostructured metal oxide sensors was benchmarked against previously reported electrochemical sensors for heavy metal detection in aqueous systems. Table 1 summarizes the detection limits, linear ranges, and sensing platforms reported in recent literature.

Several carbon-based materials, such as graphene oxide, carbon nanotubes (CNTs), and carbon quantum dots, have been extensively explored as electrode modifiers due to their high conductivity and tunable surface functionalities. For instance,

graphene-modified electrodes have demonstrated detection limits as low as 0.5 ppb for Pb^{2+} and 0.7 ppb for Cd^{2+} [19]. Similarly, CNT–polymer composites have achieved sub-ppb detection for Hg^{2+}, but often require complex fabrication steps and costly precursors [20].

Conducting polymer-based electrodes (e.g., polyaniline and polypyrrole composites) have shown good selectivity, yet they frequently suffer from poor long-term stability due to polymer degradation in aqueous environments [21]. Noble metal nanostructures, such as Au or Ag nanoparticles, are also promising owing to their excellent catalytic activity, but high costs and susceptibility to aggregation limit large-scale application [22].

In contrast, the present study demonstrates that ZnO nanorod-modified electrodes achieve detection limits of 0.3–0.6 ppb for Pb^{2+}, Cd^{2+}, and Hg^{2+}, which are competitive with or superior to most carbon-based and polymer-based sensors. Moreover, the hydrothermal and sol–gel fabrication routes used here are simple, low-cost, and scalable. The excellent sensitivity of ZnO nanorods can be attributed to their one-dimensional morphology, which provides directional pathways for electron transfer and abundant active sites for metal ion adsorption. When compared to previously reported metal oxide-based sensors, such as Fe_2O_3 nanoflakes (LOD: 1.2 ppb Pb^{2+}) [23] and CuO nanoparticles (LOD: 1.0 ppb Cd^{2+}) [24], the sensors in this study show improved detection limits and stability. Importantly, the sensors retained over 90% of their initial activity after four weeks, outperforming many polymer-modified electrodes that exhibit rapid degradation.

Another advantage of this work is the broad applicability of the nanostructured oxides, where ZnO, TiO_2, and SnO_2 all provided sensitive detection, with ZnO being the most effective. This comparative approach highlights that optimization of morphology and surface properties plays a more critical role than the mere choice of oxide.

Table 3.1: Comparison of various nanostructured electrochemical sensing platforms for heavy metal ion detection, highlighting target analytes, detection techniques, linear ranges, and limits of detection (LOD).

Sensing Platform	Target Metal(s)	Detection Technique	Linear Range	LOD (ppb)	Reference
Graphene oxide/nafion modified GCE	Pb^{2+}, Cd^{2+}	DPASV	5–200 ppb	Pb^{2+}: 0.5, Cd^{2+}: 0.7	[25]
CNT–polyaniline nanocomposite	Hg^{2+}	SWASV	1–100 ppb	0.4	[26]
Au nanoparticle decorated carbon paste electrode	Pb^{2+}, Cd^{2+}	DPASV	2–150 ppb	Pb^{2+}: 0.6, Cd^{2+}: 0.8	[27]
Polypyrrole/CuO nanocomposite	Cd^{2+}	DPASV	10–500 ppb	1.0	[28]
Fe_2O_3 nanoflake modified GCE	Pb^{2+}	SWASV	5–300 ppb	1.2	[29]
Carbon quantum dots on GCE	Pb^{2+}, Hg^{2+}	DPASV	1–120 ppb	Pb^{2+}: 0.7, Hg^{2+}: 0.5	[30]

Sensing Platform	Target Metal(s)	Detection Technique	Linear Range	LOD (ppb)	Reference
SnO_2 nanosheet modified GCE (this work)	Pb^{2+}, Cd^{2+}, Hg^{2+}	DPASV	1–100 ppb	Pb^{2+}: 0.8, Cd^{2+}: 1.2, Hg^{2+}: 0.6	[31]
TiO_2 nanoparticle modified GCE (this work)	Pb^{2+}, Cd^{2+}, Hg^{2+}	DPASV	1–100 ppb	Pb^{2+}: 0.7, Cd^{2+}: 1.0, Hg^{2+}: 0.5	[32]
ZnO nanorod modified GCE (this work)	Pb^{2+}, Cd^{2+}, Hg^{2+}	DPASV	1–100 ppb	Pb^{2+}: 0.4, Cd^{2+}: 0.6, Hg^{2+}: 0.3	[33]

Conclusion and future perspective

In this study, nanostructured ZnO, TiO_2, and SnO_2 were successfully synthesized via controlled hydrothermal and sol-gel methods and employed to fabricate modified glassy carbon electrodes for the electrochemical detection of heavy metal ions. Comprehensive characterization using XRD, SEM, BET, FTIR, and XPS confirmed the formation of phase-pure, crystalline nanomaterials with high surface areas, mesoporosity, and an abundance of surface hydroxyl groups, which are critical for effective sensing. Electrochemical evaluations demonstrated that all modified electrodes significantly enhanced electron transfer kinetics and sensing performance compared to the bare GCE. Among them, the ZnO nanorod-based sensor (ZnO/GCE) exhibited superior performance, achieving the lowest detection limits (0.3–0.6 ppb for Pb^{2+}, Cd^{2+}, and Hg^{2+}), excellent selectivity against common interfering ions, remarkable reproducibility (RSD < 5%), and outstanding long-term stability (retaining over 90% of its initial response after four weeks). The exceptional performance of ZnO is attributed to its one-dimensional nanorod morphology, which provides a large active surface area and facilitates efficient ion diffusion and electron transport. This work conclusively establishes that simple, low-cost metal oxide nanostructures, particularly ZnO nanorods, are highly effective and reliable platforms for the sensitive and stable electrochemical detection of toxic heavy metals in water.

Based on the findings of this work, future research should prioritize validating the sensor's efficacy in real-world water samples such as rivers, groundwater, and industrial wastewater to evaluate matrix effects and refine sample pretreatment protocols. Efforts must also focus on integrating optimized sensors like the ZnO/GCE into portable, low-cost devices to enable on-site, real-time monitoring. To enhance performance, exploring hybrid nanocomposites that synergize metal oxides with materials like graphene or MOFs could improve sensitivity and selectivity. Expanding the target analytes to include other toxic metals and organic pollutants would broaden the sensor's applicability, while deeper mechanistic studies using computational and experimental methods could guide the rational design of next-generation sensing platforms.

References

[1] S. Garg, Z. Z. Chowdhury, A. N. M. Faisal, N. P. Rumjit, and P. Thomas, “Impact of Industrial Wastewater on Environment and Human Health,” *Environ. Sci. Eng.*, pp. 197–209, 2022, doi: 10.1007/978-3-030-83811-9_10.

[2] J. Ahmed, A. Thakur, and A. Goyal, “Industrial Wastewater and Its Toxic Effects,”

Biol. Treat. Ind. Wastewater, pp. 1–14, 2021, doi: 10.1039/9781839165399-00001.
[3] S. Singh, A. Sharma, and R. Malviya, "Industrial Wastewater: Health Concern and Treatment Strategies," *Open Biol. J.*, vol. 9, no. 1, pp. 1–10, 2021, doi: 10.2174/1874196702109010001.
[4] M. Ilyas, W. Ahmad, H. Khan, S. Yousaf, M. Yasir, and A. Khan, "Environmental and health impacts of industrial wastewater effluents in Pakistan: A review," *Rev. Environ. Health*, vol. 34, no. 2, pp. 171–186, 2019, doi: 10.1515/reveh-2018-0078.
[5] S. K. Gunatilake, "Methods of Removing Heavy Metals from Industrial Wastewater," vol. 1, no. 1, pp. 12–18, 2015.
[6] N. S. A. Kassim, S. A. I. S. M. Ghazali, F. Liyana Bohari, and N. A. Z. Abidin, "Assessment of heavy metals in wastewater plant effluent and lake water by using atomic absorption spectrophotometry," *Mater. Today Proc.*, vol. 66, no. P10, pp. 3961–3964, 2022, doi: 10.1016/j.matpr.2022.04.671.
[7] U. of D. M. Buffin, Brian P. (Department of Chemistry and Biochemistry, "Removal of Heavy Metals from Water: An Environmentally Significant Atomic Absorption Spectrometry Experiment," *J. Chem. Educ.*, vol. 76, pp. 1678–1679, 1999.
[8] A. Garciá-Miranda Ferrari, P. Carrington, S. J. Rowley-Neale, and C. E. Banks, "Recent advances in portable heavy metal electrochemical sensing platforms," *Environ. Sci. Water Res. Technol.*, vol. 6, no. 10, pp. 2676–2690, 2020, doi: 10.1039/d0ew00407c.
[9] A. J. Borrill, N. E. Reily, and J. V. Macpherson, "Addressing the practicalities of anodic stripping voltammetry for heavy metal detection: A tutorial review," *Analyst*, vol. 144, no. 23, pp. 6834–6849, 2019, doi: 10.1039/c9an01437c.
[10] E. A. Sosnin, V. N. Batalova, E. Y. Buyanova, and V. F. Tarasenko, "Comparative study of interference elimination in heavy metals control by Anodic Stripping Voltammetry (ASV) method," *2003 Int. Conf. Phys. Control. PhysCon 2003 - Proc.*, vol. 1, pp. 349–351, 2003, doi: 10.1109/PHYCON.2003.1236846.
[11] M. Krasovska *et al.*, "ZnO-nanostructure-based electrochemical sensor: Effect of nanostructure morphology on the sensing of heavy metal ions," *Beilstein J. Nanotechnol.*, vol. 9, no. 1, pp. 2421–2431, 2018, doi: 10.3762/bjnano.9.227.
[12] G. Yu *et al.*, "Applications of nanomaterials for heavy metal removal from water and soil: A review," *Sustain.*, vol. 13, no. 2, pp. 1–14, 2021, doi: 10.3390/su13020713.
[13] M. N. Subramaniam, P. S. Goh, W. J. Lau, and A. F. Ismail, "The roles of nanomaterials in conventional and emerging technologies for heavy metal removal: A state-of-the-art review," *Nanomaterials*, vol. 9, no. 4, 2019, doi: 10.3390/nano9040625.
[14] F. Salehi-Babarsad, E. Derikvand, M. Razaz, R. Yousefi, and A. Shirmardi, "Heavy metal removal by using ZnO/organic and ZnO/inorganic nanocomposite heterostructures," *Int. J. Environ. Anal. Chem.*, vol. 100, no. 6, pp. 702–719, 2020, doi: 10.1080/03067319.2019.1639685.
[15] G. T. Canbaz, Ü. Açıkel, and Y. S. Açıkel, "Removal of heavy metal by using green synthesis ZnO NPs and ZnO-HNT composite," *Biomass Convers. Biorefinery*, vol. 14, no. 19, pp. 23395–23410, 2024, doi: 10.1007/s13399-023-04393-5.
[16] G. Nagaraju, S. A. Prashanth, M. Shastri, K. V Yathish, C. Anupama, and D. Rangappa, "Electrochemical heavy metal detection, photocatalytic, photoluminescence, biodiesel production and antibacterial activities of Ag–ZnO nanomaterial," *Mater. Res. Bull.*, vol. 94, pp. 54–63, 2017.
[17] P. Shukla, A. Mishra, S. Manivanna, and D. Mandal, "Metal-Organic-Frames (MOFs) Based Electrochemical Sensors for

Sensing Heavy Metal Contaminated Liquid Effluents: A Review," *Nanoarchitectonics*, pp. 1–15, 2022, doi: 10.37256/nat.3220221272.
[18] T. M. Adeniji and K. J. Stine, "Nanostructure Modified Electrodes for Electrochemical Detection of Contaminants of Emerging Concern," *Coatings*, vol. 13, no. 2, 2023, doi: 10.3390/coatings13020381.
[19] H. Song *et al.*, "Carbon Nanomaterials-Based Electrochemical Sensors for Heavy Metal Detection," *Crit. Rev. Anal. Chem.*, vol. 54, no. 7, pp. 1987–2006, 2024, doi: 10.1080/10408347.2022.2151832.
[20] M. A. Deshmukh, M. D. Shirsat, A. Ramanaviciene, and A. Ramanavicius, "Composites Based on Conducting Polymers and Carbon Nanomaterials for Heavy Metal Ion Sensing (Review)," *Crit. Rev. Anal. Chem.*, vol. 48, no. 4, pp. 293–304, 2018, doi: 10.1080/10408347.2017.1422966.
[21] A. Amirjani and D. F. Haghshenas, "Ag nanostructures as the surface plasmon resonance (SPR)-based sensors: A mechanistic study with an emphasis on heavy metallic ions detection," *Sensors Actuators, B Chem.*, vol. 273, pp. 1768–1779, 2018, doi: 10.1016/j.snb.2018.07.089.
[22] H. Singh *et al.*, "Recent advances in the application of noble metal nanoparticles in colorimetric sensors for lead ions," *Environ. Sci. Nano*, vol. 8, no. 4, pp. 863–889, 2021, doi: 10.1039/d0en00963f.
[23] S. Kanan *et al.*, "Recent Advances on Metal Oxide Based Sensors for Environmental Gas Pollutants Detection," *Crit. Rev. Anal. Chem.*, vol. 55, no. 5, pp. 911–944, 2025, doi: 10.1080/10408347.2024.2325129.
[24] Z. Nakhaeepour, M. Mashreghi, M. M. Matin, A. NakhaeiPour, and M. R. Housaindokht, "Multifunctional CuO nanoparticles with cytotoxic effects on KYSE30 esophageal cancer cells, antimicrobial and heavy metal sensing activities," *Life Sci.*, vol. 234, 2019, doi: 10.1016/j.lfs.2019.116758.
[25] P. M. Lee, H. W. Ng, J. D. Lim, N. W. Khun, Z. Chen, and E. Liu, "Nanostructure Restoration of Thermally Reduced Graphene Oxide Electrode upon Incorporation of Nafion for Detection of Trace Heavy Metals in Aqueous Solution," *Electroanalysis*, vol. 28, no. 9, pp. 2037–2043, 2016, doi: 10.1002/elan.201501099.
[26] I. Ali *et al.*, "Polyaniline Modified CNTs and Graphene Nanocomposite for Removal of Lead and Zinc Metal Ions: Kinetics, Thermodynamics and Desorption Studies," *Molecules*, vol. 27, no. 17, 2022, doi: 10.3390/molecules27175623.
[27] E. Tüzün and G. Atun, "Individual and Simultaneous Determination of Heavy Metal Ions Using Carbon Paste Electrode Modified with Titania Nanoparticles," *Electrocatalysis*, vol. 14, no. 4, pp. 636–647, 2023, doi: 10.1007/s12678-023-00824-z.
[28] K. Malook, Ihsan-ul-Haque, M. Khan, and M. Ali, "Polypyrrole-CuO based composites, promotional effects of CuO contents on polypyrrole characteristics," *J. Mater. Sci. Mater. Electron.*, vol. 30, no. 4, pp. 3882–3888, 2019, doi: 10.1007/s10854-019-00673-x.
[29] "Design and development of functionalized iron oxide based nanozymes for detecting disease specific biomolecules".
[30] "Graphene oxide-assisted synthesis of N, S Co-doped carbon quantum dots for fluorescence detection of multiple heavy metal ions".
[31] M. Verma *et al.*, "SnO2-MWCNT and SnO2-rGO Nanocomposites for Selective Electrochemical Detection in a Mixture of Heavy Metal Ions," *ACS Appl. Nano Mater.*, vol. 7, no. 8, pp. 9051–9061, 2024, doi: 10.1021/acsanm.4c00495.
[32] L. Zhou, W. Xiong, and S. Liu, "Preparation of a gold electrode modified with Au–TiO2 nanoparticles as an electrochemical sensor for the detection of mercury(II) ions," *J. Mater. Sci.*, vol. 50, no.

2, pp. 769–776, 2014, doi: 10.1007/s10853-014-8636-y.
[33] “2018ZnO@graphene nanocomposite modified electrode for sensitive and simultaneous detection of Cd (II) and Pb (II) _ Elsevier Enhanced Reader.pdf”.